

# Development of Receptive Fields in a Closed-Loop Behavioural System

Tomas Kulvicius<sup>a</sup> & Bernd Porr<sup>b</sup> & Florentin Wörgötter<sup>a,c</sup>

<sup>a</sup>*Bernstein Center of Computational Neuroscience, University Göttingen,  
Bunsenstr. 10, 37073 Göttingen, Germany*

<sup>b</sup>*Department of Electronics & Electrical Engineering, University of Glasgow,  
GT12 8LT Glasgow, UK*

<sup>c</sup>*Computational Neuroscience, University of Stirling, FK9 4LR Stirling, UK*

---

## Abstract

Recently it has been pointed out that in simple animals like flies a motor neuron can have a visual receptive field [1]. Such receptive fields directly generate behaviour which, through closing the perception-action loop, will feed back to the sensors again. In more complex animals an increasingly complex hierarchy of visual receptive fields exists from early to higher visual areas, where visual input becomes more and more indirect. Here we will show that it is possible to develop receptive fields in simple behavioural systems by ways of a temporal sequence learning algorithm. The main goal is to demonstrate that learning generates stable behaviour and that the resulting receptive fields are also stable as soon as the newly learnt behaviour is successful.

*Key words:* Receptive fields, Temporal sequence learning, Closed loop

---

## 1 Introduction

A receptive field (RF) of a given neuron is that particular surface area of sensor organ from which responses can be elicited. Sensory inputs should be triggered in order to get response from the neuron. We will apply temporal sequence learning to a driving robot that is supposed to learn to better follow a curvy line painted on the ground. We will demonstrate: 1) That it is possible

---

*Email addresses:* [tomas@chaos.gwdg.de](mailto:tomas@chaos.gwdg.de) (Tomas Kulvicius),  
[b.porr@elec.gla.ac.uk](mailto:b.porr@elec.gla.ac.uk) (Bernd Porr), [worgott@chaos.gwdg.de](mailto:worgott@chaos.gwdg.de) (Florentin Wörgötter).

with such architectures to generate “receptive fields” from sensory inputs. 2) That the output of these RFs can drive the motors of the robot in order to create better and more stable behaviour, (which in turn influences its sensor inputs) and 3) that RF development will stop as soon as the system has obtained this behavioural stability after learning. Furthermore we will show (4) that it is possible to design simple chains of such learning units while at the same time still guaranteeing behavioural stability. The central goal of this approach is to demonstrate that direct sensor-motor coupling in a very simple architecture can lead to the generation of stable structural elements and simultaneously to stable behaviour without additional assumptions, while it is possible to gradually extend such architectures towards lattices without the need for additional free parameters.

## 2 Methods

The learner (open loop case) has inputs  $x_j$  which feed into a summation unit  $v$  (see Fig. 1 B). The output is calculated by  $v = \sum_j \rho_j u_j$ , where  $u = h * x$  is a convolution of input  $x$  with resonator  $h$ . We define  $h(t) = \frac{1}{b} e^{at} \sin(bt)$ ,  $a = -\pi f/Q$  and  $b = \sqrt{(2\pi f)^2 - a^2}$ , with  $f$  the frequency and  $Q > 0.5$  the damping. The delay between  $x_0$  and  $x_1$  depends on the speed of the robot. To accommodate some variability,  $x_1$  is fanned out and fed into a filterbank of different filters  $h$  as indicated by the dashed lines. The number of filters is not critical and we use 10. The robot’s base speed of  $0.125 \text{ m/s}$  together with the camera frame rate of  $25 \text{ Hz}$  used in all experiments leads to  $f_{1,k} = 2.5/k \text{ Hz}$ ,  $k = 1, \dots, 10$  for the filterbank in the  $x_1$  pathway. Frequency of the  $x_0$  pathway was  $f_0 = 1.25 \text{ Hz}$ . Damping parameters of all filters were  $Q = 0.6$ . Weights change according to an input-input correlation rule:  $\dot{\rho}_j = \mu u_j \dot{u}_0$ ,  $j > 0$ . The behaviour of this rule and its convergence properties are discussed in [2]. Initially the system is set up only to react to the near-sense  $x_0$  by ways of a reflex. The late and weak reflex response by itself is not enough to assure line-following behaviour; therefore the robot misses the line whenever it drives without learning. The convolution of input signals with resonators allows correlating temporally non-overlapping signals allowing to apply temporal difference learning. Goal of the learning is to grow  $w_1$  that the learner can use the earlier signal at  $x_1$  to generate an anticipatory reaction. Learning stops and the weights stabilise at the condition  $x_0 = 0$  when the reflex is not triggered anymore (i.e. the system does not receive input from the near-sense  $x_0 = 0$ ). We used a small (diameter of 18 cm) two-wheeled Rug Warrior Pro driving robot for investigation which is shown in Fig. 1 A. We use a line-following task to develop RFs in a closed loop scenario where a reflexive reaction ( $x_0$ ) and predictive reactions ( $x_1$ ) are generated from sensor fields in the image of a forward pointing camera. RFs  $x_1^{L,R}$  (Fig. 2 A) in pixel-

lines more at the top correspond to the far future of the robot's trajectory and act predictive in comparison to sensor fields  $x_0^{L,R}$  at the bottom, whereas RFs  $x_2^{L,R}$  (Fig. 3 A) act predictive in comparison to RFs  $x_1^{L,R}$ . Two different neuronal setups of the robot are presented in Fig. 1 C. The unchained neuronal setup, called *simple*, is shown in the dashed box of Fig. 1 C. It has one neuron on which signals from both sides of the view-field converge. Inputs from the left  $x^L$  side are negative whereas inputs from the right side  $x^R$  are positive. The chained neuronal setup, called the *linear-chain*, is presented in Fig. 1 C. There is one reflex input  $x_0$  and two predictive inputs  $x_1$  and  $x_2$ . Output  $v_\beta$  is used as the reflex input of the neuron  $\gamma$ . The weights  $\rho_0^{\beta,\gamma}$  are set to a fixed value 1, all other weights are initially 0. The robot has a left and a right motor, which receive a certain forward drive leading to a constant speed of  $S_{basic} = 0.125 \text{ m/s}$  in all experiments. This signal is modified by braking ( $|v^\beta|$ ) and steering ( $\pm v^\beta$ ) according to:  $S^{L,R} = S_{basic} - |v^\beta| \pm v^\beta$ , where for the left motor we use "-" and for the right "+" . For the chained architecture, we use  $v^\gamma$  instead of  $v^\beta$  in the equation.

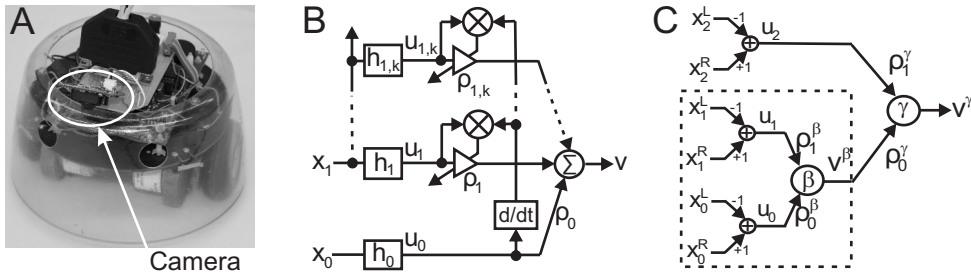


Fig. 1. **A)** Picture of the robot. **B)** Schematic diagram of the learning system in the open-loop. Components of the learning system. Inputs  $x$ , resonator filters  $h$ , connection weights  $\rho$ , output  $v$ . The symbol  $\otimes$  denotes a multiplication,  $d/dt$  a temporal derivative. The amplifier symbol stands for a variable connection weight. Dashed lines indicate that input  $x_1$  is fed into a filterbank. **C)** The neuronal architectures of the learning system: *simple* (dashed box) and *linear-chain*.

### 3 Results

Results of the RFs development using the simple neuronal setup on different tracks (track length is about 2 m) are shown in Fig. 2. A total of 225 sensor fields of 1 pixel were used for the far-sensor (Fig. 2 A). The resulting right RFs  $x_1^R$  is shown in Fig. 2 B-D where light colour correspond to strong sub-fields and dark to weak sub-fields. The left RF is the mirror image of the right one due to the symmetry of the learning setup. Obtained RFs do not change as soon as the appropriate behaviour is achieved and the initially existing reflex is no longer triggered ( $x_0 = 0$ ). Results of the RF development using the linear-chain are shown in Fig. 3. Here we used 100 sensor fields of 1 pixel for

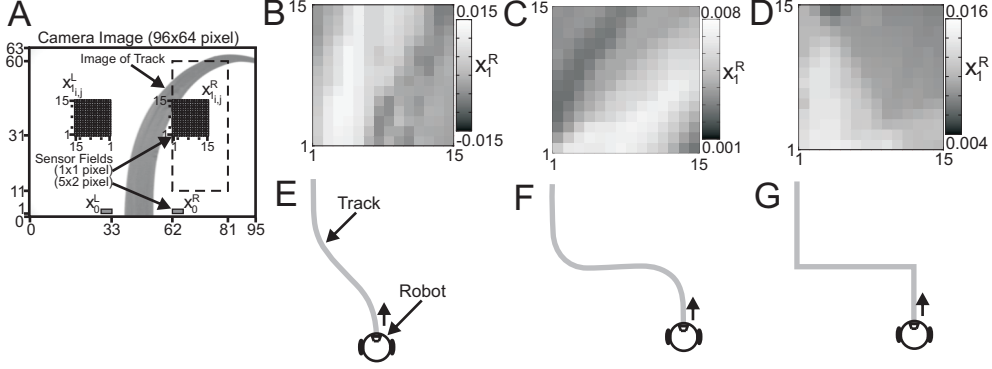


Fig. 2. Results of the RF development using the simple neuronal setup on different tracks. **A)** Physical setup. The RF positions on the image are denoted by  $x_{1,i,j}^{L,R}$  where  $i, j$  are the indices of the RF pixels and sensor field positions  $x_0^{L,R}$ . **B, D)** Right RFs obtained from the simple setup. The diagrams show the summed weights  $\sum_{k=1}^{10} \rho_{1,i,j,k}^\beta$  over all 10 filters in the filterbank which receive inputs from the corresponding predictor  $x_{1,i,j}^R$ . **B)** Results for the shallow track (**E**). Learning rate was  $\mu = 1.7 \times 10^{-8}$ . Learning stopped after three trials (see video rf-shallow.mpg, please download at <http://www.chaos.gwdg.de/~tomas/drv/>). **C)** Results for the intermediately steep track (**F**). Learning rate was  $\mu = 10^{-8}$ . Learning stopped after four trials (see video rf-225.mpg). Results for the sharp track (**G**). Learning rate was  $\mu = 1.7 \times 10^{-8}$ . Learning stopped after six trials (see video rf-sharp.mpg).

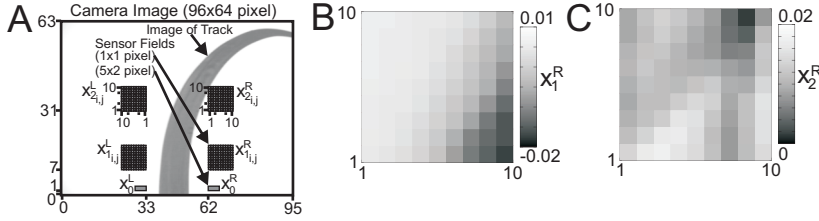


Fig. 3. Results of the RF development using the linear-chain setup. **A)** Physical setup. The different RF positions on the image are denoted by  $x_{1,2,i,j}^{L,R}$  where  $i, j$  are the indices of the RF pixels and sensor field positions  $x_0^{L,R}$ . **B, C)** Right RFs obtained from the linear chain on intermediate track. **B)** Summed weights  $\sum_{k=1}^{10} \rho_{1,i,j,k}^\beta$  over all 10 filters in the filterbank which receive inputs from the corresponding predictor  $x_{1,i,j}^R$  and **C)** summed weights  $\sum_{k=1}^{10} \rho_{1,i,j,k}^\gamma$  over all 10 filters in the filterbank which receive inputs from the corresponding predictor  $x_{2,i,j}^R$ . Learning rate was  $\mu = 2 \times 10^{-8}$ .

both predictors (Fig. 3 A). Results for the development of the primary RF of predictor  $x_1^R$  are presented in Fig. 3 B and for the secondary RF of predictor  $x_2^R$  in Fig. 3 C. Both fields are different: the secondary field  $x_2^R$  is noisier than the primary  $x_1^R$ . This is to be expected as a consequence of the large amount of indirect input  $v^\beta$  that it receives on its reflex line.

## 4 Discussion

The development of visual RFs has been in the centre of research interest during the last decade and it had been shown that cortical RFs can develop following a sparseness principle and essentially implementing independent component analysis [3,4]. However, only very few attempts exist to develop RFs from signals of a behaving agent [5], most notably in robot-models of hippocampal place fields [6]. These models differ strongly from our approach because they are still open loop. This is different for a recent study by [7] who were able to close the loop and derive path-following behaviour in a robot that is driven by a complex multi-layer neuronal system supposed to mimic parts of the cerebellar system. This is done by the neurons in the simulated Inferior Olive which adapt following a Hebbian learning rule. Synaptic weight matrices (RFs), develop at several stages in the network, but it appears that this type of learning will not lead to their final stabilisation. By applying temporal sequence learning we developed RFs in a closed-loop behavioural task. We also showed that it is possible to generate and stabilise secondary RFs in a closed loop context.

## References

- [1] H. G. Krapp, S. J. Huston, Encoding self-motion: From visual receptive fields to motor neuron response maps, in: H. Zimmermann, K. Kriegstein (Eds.), Proceedings of the 6th Meeting of the German Neuroscience Society / 30th Göttingen Neurobiology Conference 2005, Göttingen, 2005, pp. S16–3.
- [2] B. Porr, F. Wörgötter, Strongly improved stability and faster convergence of temporal sequence learning by utilising input correlations only, Neural Comp. (in press).
- [3] B. A. Olshausen, D. J. Field, Emergence of simple-cell receptive field properties by learning a sparse code for natural images, Nature 381 (6583) (1996) 607–609.
- [4] A. J. Bell, T. J. Sejnowski, The "independent components" of natural scenes are edge filters, Vision Res 37 (23) (1997) 3327–3338.
- [5] W. Einhäuser, C. Kayser, P. König, K. P. Körding, Learning the invariance properties of complex cells from their responses to natural stimuli, Eur J Neurosci 15 (3) (2002) 475–486.
- [6] A. Arleo, W. Gerstner, Spatial cognition and neuro-mimetic navigation: a model of hippocampal place cell activity, Biol Cybern 83 (3) (2000) 287–299.
- [7] J. L. McKinstry, G. M. Edelman, J. L. Krichmar, A cerebellar model for predictive motor control tested in a brain-based device, Proc Natl Acad Sci U S A 103 (9) (2006) 3387–3392.